CORE
Metadata, citation and similar papers at core.ac.uk
Provided by University of Queensland eSpace

Online available since 2011/Jun/30 at www.scientific.net
© (2011) Trans Tech Publications, Switzerland
doi:10.4028/www.scientific.net/SSP.172-174.1307

click for feedback
consult - comment - contact

Heteroepitaxy crystallography in low dimensional nanostructures

Dong Qiu[1,2, a], Mingxing Zhang[1,2,b] and Patrick Kelly[1,c]

[1] School of Mechanical and Mining Engineering, University of Queensland, St. Lucia, Queensland 4072, Australia
[2] ARC Centre of Excellence for Design in Light Metals, Australia

[a] d.qiu@uq.edu.au, [b] mingxing.zhang@uq.edu.au, [c] p.kelly@uq.edu.au

Key words: Crystallography; heteroepitaxy; nanowires; orientation relationship; substrate design.

Abstract. Low dimensional nanostructures, e.g. nanowires, self-assembled through heteroepitaxy, present a variety of crystallographic features that do not always follow conventional V-W or S-K growth mode. Applying Δ**g** parallelism rules and edge-to-edge matching (E2EM) model in β-$DySi_2$/Si and $CoSi_2$/Si systems provides a better understanding of the natural preference of the interface orientation and the orientation relationship (OR) during heteroepitaxial growth. This may help improving the quality of nanowires through optimizing the substrate orientation.

Introduction

The development of electronic and photonic devices based on low-dimensional semiconductor materials, including thin films, nanowires and quantum dots, has been one of the most blooming fields in the 21st century to fulfil the growing demand of information industry. A great many nanostructures are fabricated via heteroepitaxy techniques, such as MBE and MOVPE, etc [1]. Since there is rarely perfect lattice matched substrate, the strain relaxation is a critical issue for high quality nanowires. The most prevailing modes describing the strain relaxation during heteroepitaxial growth are Volmer-Weber (V-W) mode [2] and Stranski-Krastanow (S-K) mode [3], in a system with considerable lattice mismatch involved. Both modes end up with the formation of 3-D islands instead of uniform films to reduce the strain energy of the nanostructures. The island is either elastic deformed (V-W mode) or accompanied with misfit dislocations underneath to accommodate lattice mismatch (S-K mode). In both growth modes, a certain epitaxial relationship, normally a rational orientation relationship (OR) and a low-indexed interface is presumed. However, not too much attention has been paid on how the interfacial energy between the substrate and nanostructures, the structural component (E_s) in particular, can be reduced through alteration of the OR and interface orientation that ends up with a long-range strain-free interface. In fact, crystallographic tilting away from the conventional texture orientation has been observed in a number of systems [4-7]. Meanwhile, recent studies have shown that large-scale, smooth and low-defect thin films can also be fabricated on inclined substrate surfaces and their performance is sometimes even better than that with the low-indexed surface [8-10].

For a better understanding of the coexistence of rational and irrational crystallographic features in heteroepitaxial growth system, Δ**g** parallelism rules [11,12] and edge-to-edge matching (E2EM) model [13,14] will be applied to β-$DySi_2$/Si and $CoSi_2$/Si nanowire systems in this paper. Since these two approaches have been well acknowledged in describing the precipitation crystallography in bulk materials, it is of great interest to see whether they are also applicable in heteroepitaxial growth systems and if yes, how they work for a given heteroepitaxial growth system.

Understanding of the crystallographic features in β-$DySi_2$/Si nanowires system

β-$DySi_2$ is a typical member in the rear-earth metal silicide family with much lower Schottky barrier height than that of the refractory metal silicide, which enables itself a good potential to be applied in semiconductor industry [15]. The self-assembled β-$DySi_2$ nanowires can grow on Si substrate with different orientations, such as Si(111), Si(001) and Si(110). The nanowires always have a preferential growth direction along $<110>_{Si}$ // $<2\bar{1}\bar{1}0>_{\beta}$; however, the HRTEM images

consult comment contact
click for feedback

All rights reserved. No part of contents of this paper may be reproduced or transmitted in any form or by any means without the written permission of TTP, www.ttp.net. (ID: 130.102.158.16-20/09/11,04:34:22)

taken along the growth direction clearly indicate the difference of cross-section profile, as shown in Figs. 1(a) and (b). The nanowires grown on Si(111) have an almost atomically flat interface parallel to the substrate [16], while a stepped interface inclined at 3~5° to the substrate was always observed on Si(001) [17,18]. A small lattice tilt of ≤1° was also observed with the Si(001) substrate [18]. In addition, previous scanning tunneling microscopy (STM) studies [19,20] showing regular trenches about 3 nm wide indicate the existence of a set of misfit dislocations along $<110>_{Si}$ // $<2\bar{1}\bar{1}0>_{\beta}$. β-$DySi_2$ nanowires grown on a Si(110) surface have the same OR with the substrate as the Si(111) case, but the interface is parallel to the plane $(111)_{Si}$ in a 'endotaxy' fashion [21].

Careful examination of the HRTEM images of β-$DySi_2$ nanowires on Si(111) [16] confirms that a set of plane pairs $(11\bar{1})_{Si}$ | $(0\bar{1}11)_{\beta}$ meeting each other at the interface $(111)_{Si}$ // $(0001)_{\beta}$ in a edge-to-edge matching manner along the $<110>_{Si}$ // $<2\bar{1}\bar{1}0>_{\beta}$ direction, as highlighted in Fig. 1(a). The same atomic row matching fashion can be also found between plane pair $(111)_{Si}$ | $(0001)_{\beta}$ when β-$DySi_2$ nanowires grow on Si(001) [17], as shown in Fig. 1(b). The above observations indicate that the E2EM model has a strong potential to be applied in this system.

The key elements in E2EM model is the *matching rows* and the *matching planes* from adjacent phases. The matching rows are required to be a pair of close packed (C.P.) rows with small interatomic spacing misfit (f_r) along each of their row directions, normally less than 10% [22]. Meanwhile, the matching planes whose edges meet at the matching rows along the interface should be C.P. or near C.P. planes in each phase. The interplanar spacing mismatch (f_d) between the matching planes is required to be less than 6% for matrix/precipitates systems [22]. It should be noted that the 6% threshold for f_d is based on the investigations in diffusional phase transformations, where the precipitate nucleus has 3D rigid-body constraints from the surrounding matrix. Large f_d values usually increase the angular discrepancy between the C.P. plane pair, which is not favoured in terms of the precipitation kinetics. In contrast, the self-assembled nanowires are constraint free along the normal to the substrate. The matching plane pairs between nanowires and their substrate do not need to maintain a near-parallel relationship. In other words, f_d is not necessary to identify the matching planes in heteroepitaxy systems. But the matching planes are still required to be C.P. planes to carry the matching rows to the interface.

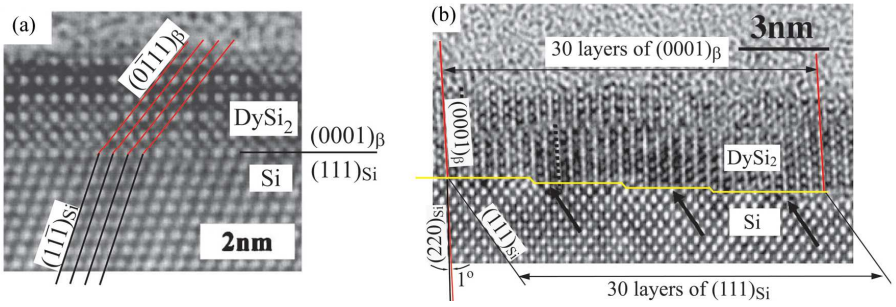

Fig. 1 Reprinted HRTEM observations [16,17] showing the cross section of $DySi_2$ nanowires on (a) Si(111) and (b) Si(001). The stepped interface in (b) is indicated by yellow broken lines.

In β-$DySi_2$/Si system, β-$DySi_2$ has a hexagonal lattice structure with lattice constants a = 0.383nm and c = 0.412nm. Two C.P. planes of β-$DySi_2$ were identified, i.e. $\{0001\}_{\beta}$ and $\{0\bar{1}11\}_{\beta}$, while only one C.P. row in a zigzag fashion along the $<2\bar{1}\bar{1}0>_{\beta}$ direction lies in both C.P. planes. The substrate material, Si has a diamond structure with $\{111\}_{Si}$ as its most C.P. plane. The only C.P. row runs along the $<110>_{Si}$ direction and it is also a zigzag row. Therefore, only one pair of zigzag C.P. rows $<2\bar{1}\bar{1}0>_{\beta}$ | $<110>_{Si}$ is available in this system. According to the lattice constants of $DySi_2$ and Si, this C.P. row pair has a very small f_r value of only 0.26% and hence is an ideal and also unique pair of matching rows to be parallel to each other. The small f_r value also means nearly full coherency between β-$DySi_2$ and Si along this pair of C.P. rows, which will be favoured during heteroepitaxial growth. This is in a good agreement with the common feature of the β-$DySi_2$ nanowires running along $<2\bar{1}\bar{1}0>_{\beta}$ // $<110>_{Si}$ no matter which substrate orientation is employed.

If we specify a particular pair of matching rows, $[2\bar{1}\bar{1}0]_\beta \mid [\bar{1}10]_{Si}$, two matching plane pairs will be $(0001)_\beta \mid (111)_{Si}$ and $(0\bar{1}11)_\beta \mid (11\bar{1})_{Si}$, respectively. By using the $\Delta\mathbf{g}$ parallelism criterion [23,24] in reciprocal space, two ORs can be determined. The first OR can be expressed as

$[2\bar{1}\bar{1}0]_\beta \parallel [\bar{1}10]_{Si}$, $(0001)_\beta$ 0.1° away from $(111)_{Si}$, $(0\bar{1}11)_\beta$ 19.4° away from $(11\bar{1})_{Si}$ (OR I)

Fig. 2(a) shows the superimposed diffraction patterns along $[2\bar{1}\bar{1}0]_\beta \parallel [\bar{1}10]_{Si}$ at OR I. The solid line segments are parallel $\Delta\mathbf{g}$ vectors connecting the $\mathbf{g}$ vectors of matching planes. The dashed line indicates the interface trace that is perpendicular to the parallel $\Delta\mathbf{g}$ vectors. The calculated interface is 0.1° away from the $(0001)_\beta$ plane and 0.2° away from the $(111)_{Si}$ plane. Since the interface is very close to the $(111)_{Si}$ plane and the $(0001)_\beta$ plane, this C.P. plane pair will serve as the terrace planes along the interface. Theoretically, the terrace will be extremely wide — up to about 90 nm — which is far beyond the scale of typical nanowires (5~10nm wide). So the actual interface should be step free and the terrace planes $(0001)_\beta \mid (111)_{Si}$ are also expected to remain parallel to save more bonding energy and hence reduce the total interface energy. In this regard, the singular interface is not only defined by two pairs of parallel $\Delta\mathbf{g}$ vectors, but also defined by the $\mathbf{g}$ vector of the C.P. planes simultaneously. This means both the $\Delta\mathbf{g}$ parallelism Rule I ($\Delta\mathbf{g} \,//\, \mathbf{g}_P$) and the Rule II ($\Delta\mathbf{g}_{P1} \,//\, \Delta\mathbf{g}_{P2}$) apply coincidently, where subscript 'P' represents the principal planes containing at least two Burgers vectors [12], which is basically equivalent to the C.P. planes who normally contains at least two sets of C.P. rows. Such an OR and the singular interface are fully consistent with the HRTM observations as shown in Fig. 1 (a).

Similarly, the second OR can be derived from the same set of $\Delta\mathbf{g}_P$ vectors. That is:

$[2\bar{1}\bar{1}0]_\beta \parallel [\bar{1}10]_{Si}$, $(0001)_\beta$ 1.3° away from $(220)_{Si}$, $(01\bar{1}0)_\beta$ 1.3° away from $(001)_{Si}$. (OR II)

Fig. 2(b) shows the superimposed diffraction patterns along $[\bar{2}110]_\beta \parallel [1\bar{1}0]_{Si}$ at OR II. The calculated interface is is 5.7° away from the $(001)_{Si}$ plane and 7.0° away from the $(01\bar{1}0)_\beta$ plane. Hence, the plane pairs of $(002)_{Si} \mid (01\bar{1}0)_\beta$ serve as the terrace plane for each phase. The comparison between Figs. 2(b) and 1(b) indicates that the crystallographic features of OR II are in good agreement with the HRTEM observations [17,18]. However, the observed misfit dislocations along the matching rows still need to justify. Because no Burger circuit disconnection between the matching plane pairs $(0001)_\beta \mid (111)_{Si}$ (see Fig. 1(b)), the observed dislocations must be secondary misfit dislocations. Extending the superimposed diffraction pattern in Fig. 2(b) at OR II, a set of characteristic triangles [12,25] can be identified with the Burger vector of the secondary misfit dislocations, $\mathbf{b}^{II}$, as shown in Fig. 3(a) where $\mathbf{b}^{II*} = \mathbf{b}^{II}/|\mathbf{b}^{II}|^2$. The corresponding interfacial structure in direct space is shown in Fig. 3(b). It clearly shows the coincidence of the steps and the secondary misfit dislocations with the average spacing of 2.8nm, which is consistent with the previous STM observation, i.e. ~3nm. It is worth mentioning that the one-to-one correspondence between the steps and dislocations at OR II is the prominent feature of the $\Delta\mathbf{g}$ parallelism Rule III ($\Delta\mathbf{g}_{P\text{-}II} \,//\, \Delta\mathbf{g}_{//}$) where $\mathbf{g}_{P\text{-}II}$ indicates the principal planes in secondary preferred state [12], i.e. the C.P. planes of the coincidence sites lattice (CSL) and $\Delta\mathbf{g}_{//}$ is one of the edges in characteristic triangles who defines the normal of the interface, as shown in Fig. 3(a). Detailed derivation of $\mathbf{b}^{II}$ and CSL at this OR can be found elsewhere [26].

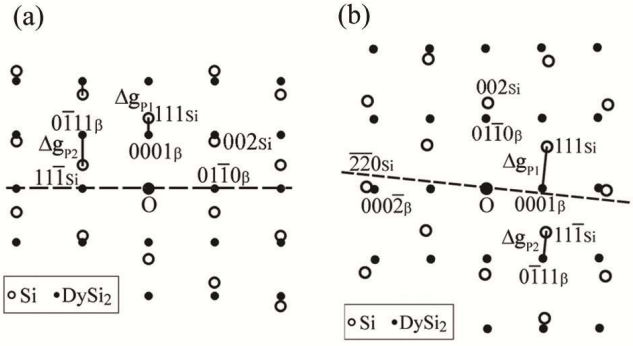

Fig. 2 Simulated diffraction patterns showing the singular interface (--) defined by two pairs of parallel $\Delta\mathbf{g}_P$'s at (a) OR I; (b) OR II

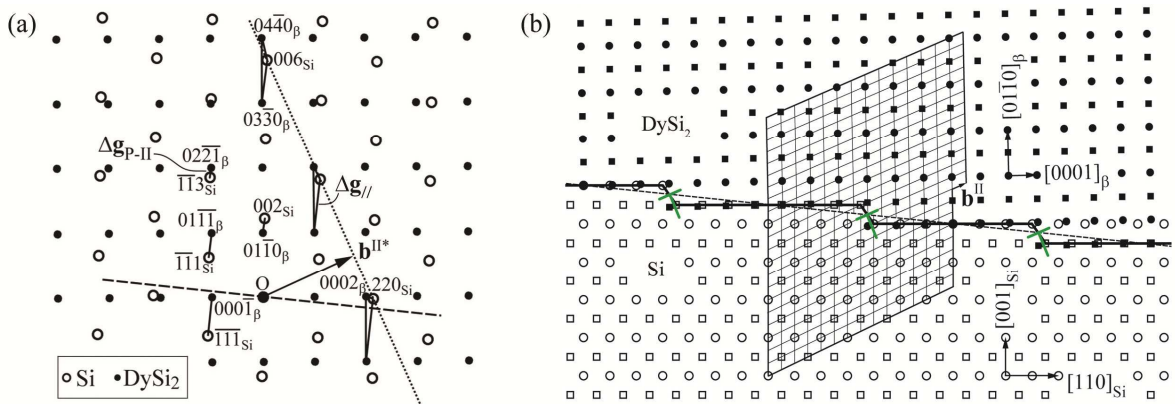

Fig. 3 (a) Extended diffraction pattern of Fig. 2(b) showing the Δ**g** parallelism Rule III at OR II; (b) interfacial structure with the one-to-one coincidence of steps and secondary dislocations (green 'T').

Understanding of the Crystallographic features in $CoSi_2$/Si nanowires system

Another interesting heteroepitaxy system is $CoSi_2$ nanowires self-assembled on Si substrate. During heteroepitaxial growth, $CoSi_2$ nanowires always hold two pseudo-twin related ORs with the Si substrate, i.e. $<01\bar{1}>_{CoSi2}$ // $<01\bar{1}>_{Si}$, $\{111\}_{CoSi2}$ // $\{111\}_{Si}$ while $\{\bar{1}11\}_{CoSi2}$ // $\{\bar{1}11\}_{Si}$ for OR A and $\{\bar{1}11\}_{CoSi2}$ // $\{\bar{5}11\}_{Si}$ for OR B [27]. Accordingly, two types of interfaces were observed. The type-A interface is a sort of coherent interface parallel to two variants of $\{111\}_{CoSi2}$ // $\{111\}_{Si}$ at OR A while type-B interface is comprised of two asymmetrical facets, i.e. $\{\bar{1}11\}_{CoSi2}$ // $\{\bar{5}11\}_{Si}$ and $\{111\}_{CoSi2}$ // $\{111\}_{Si}$. Figs. 4(b) and (c) clearly show the HRTEM observations with these two sorts of cross-section profiles [27]. Following the success of applying E2EM model in β-$DySi_2$/Si system, we repeat the analysis procedure as above mentioned, but in $CoSi_2$/Si system.

$CoSi_2$ has an fcc lattice (CaF_2 structure) with the lattice constants of 0.536 nm, which is slightly smaller than that of the substrate material, Si (a_{Si} = 0.540 nm). Hence, they have a pair of C.P. rows along $<01\bar{1}>_{CoSi2}$ | $<01\bar{1}>_{Si}$ with very small f_r value of only 0.7% – an perfect matching row pair. Meanwhile, the matching plane pairs come from the C.P. plane family of $\{111\}_{CoSi2}$ | $\{111\}_{Si}$. If we specify the matching row as $[01\bar{1}]_{CoSi2}$ | $[01\bar{1}]_{Si}$, two matching plane pairs will be $(111)_{CoSi2}$ | $(111)_{Si}$ and $(1\bar{1}\bar{1})_{CoSi2}$ | $(1\bar{1}\bar{1})_{Si}$, respectively. However, no OR can be determined meeting the parallelism of these two $\Delta\mathbf{g}_P$ vectors. The isotropic lattice correspondence between the $CoSi_2$ and Si substrate indicates it is impossible to find a direction keeping invariant since all principal strains are lower than 1 during the formation of $CoSi_2$ nanowires. In this case, the atomic row matching cannot be realized across the interface, and the Δ**g** parallelism Rule II or III is not applicable either. Instead, the Δ**g** parallelism Rule I (Δ**g** // $\mathbf{g}_P$) is still applicable.

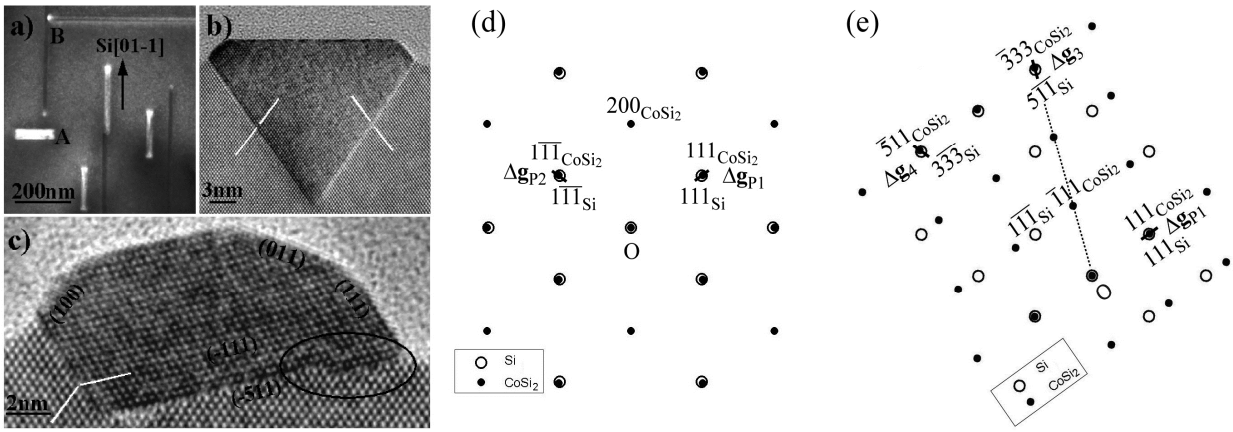

Fig. 4 (a) Plan-view TEM showing $CoSi_2$ nanowires [27]; Reprinted HRTEM cross-sections along $[01\bar{1}]_{Si}$ of (b) type-A interface and (c) type-B interface [27]; Superimposed diffraction patterns at (d) OR A and (e) OR B showing a series of single Δ**g** vectors defining the type-A and -B interfaces.

Fig. 4(d) shows the superimposed diffraction patterns along $[01\bar{1}]_{CoSi2}$ // $[01\bar{1}]_{Si}$ at OR A. We can find two $\Delta\mathbf{g}_P$ vectors connecting the $\mathbf{g}_P$ vectors of each C.P. plane pair are parallel to the $\mathbf{g}_P$ vectors themselves, respectively. Namely, $\Delta\mathbf{g}_{P1}$ // $\mathbf{g}_{(111)CoSi2}$ and $\Delta\mathbf{g}_{P2}$ // $\mathbf{g}_{(1\,\bar{1}\,\bar{1})CoSi2}$. These two $\Delta\mathbf{g}_P$ vectors just define the two type-A facets shown in Fig. 4(b). If we turn the C.P. row direction of $CoSi_2$ by 180 °, OR A will be changed to OR B and the associated superimposed diffraction patterns along $[0\bar{1}1]_{CoSi2}$ // $[01\bar{1}]_{Si}$ is shown in Fig. 4(e). Whilst $\Delta\mathbf{g}_{P1}$ is still parallel to $\mathbf{g}_{(111)CoSi2}$, defining the minor facet of type-B interface, $\Delta\mathbf{g}_{P2}$ is not parallel to $\mathbf{g}_{(\bar{1}\,\bar{1}1)CoSi2}$ due to the asymmetry of the diffraction pattern. A new $\Delta\mathbf{g}$ vector, denoted by $\Delta\mathbf{g}_3 = \mathbf{g}_{(\bar{3}33)CoSi2} - \mathbf{g}_{(5\bar{1}\,\bar{1})Si}$ parallels $\mathbf{g}_{(\bar{1}11)CoSi2}$. The interface defined by $\Delta\mathbf{g}_3$ is fully consistent with the major facet of type-B interface shown in Fig. 4(c). Another $\Delta\mathbf{g}$ vector, denoted by $\Delta\mathbf{g}_4 = \mathbf{g}_{(\bar{5}11)CoSi2} - \mathbf{g}_{(3\bar{3}\bar{3})Si}$, which parallels $\mathbf{g}_{(1\bar{1}\,\bar{1})Si}$ also defines a singular interface candidate; however it has never been reported yet. This indicates the step-free interface in terms of $CoSi_2$ is predominant rather than Si in this system.

Discussion

The interface with E2EM features means the adjacent phases share the common matching rows at the interface, and hence the long-range strain normal to the matching rows is fully relaxed. The misfit strain is confined only along the matching row direction. A single set of misfit dislocations with their Burger vector parallel to the matching row direction is enough to accommodate the lattice misfit at the interface. Hence, it is in essence consistent with the *second* optimum conditions for singular interface, i.e. elimination of the misfit dislocations in one direction [12]. However, in the β-$DySi_2$/Si system, the interface at OR I is also step-free within the scale of the nanowires' width, meeting the *first* optimum condition of the singular interface, i.e. elimination of steps along the interface. Similarly, the interface at OR II presents the one-to-one correspondence between atomic steps and secondary misfit dislocations that reduces the density of total line defects along the interface, meeting the *third* optimum condition of the singular interface [12]. This indicates that the nanowires and their substrate always yield themselves to meet the optimum conditions of singular interfaces as more as possible to minimize the interfacial energy during heteroepitaxial growth. However, from mathematical point-of-view, not each optimum condition can be satisfied for a given heteroepitaxy system. If the E2EM features can be realized by finding two pairs of parallel $\Delta\mathbf{g}_P$ vectors connecting the $\mathbf{g}_P$ vectors of matching planes along the zone axis of matching rows, the singular interface is always defined by the parallel $\Delta\mathbf{g}_P$ vectors. Generally, the $\Delta\mathbf{g}$ parallelism criterion leads to more than one pair of OR and interface orientation, such as OR I and II in β-$DySi_2$/Si system. The low-indexed interface is normally more energetically favorable than the high-indexed one due to the lower density of steps with localized distortion when the substrate is far from either singular interface in terms of their orientation, as we see the interface $(0001)_\beta$ // $(111)_{Si}$ when β-$DySi_2$ nanowires grow on the Si(110) substrate [21]. Meanwhile, in certain heteroepitaxy systems, in particular when the adjacent phases have isotropic unit cells with slightly different lattice constants, such as $CoSi_2$/Si system in the above example, the E2EM model may be not applicable due to the isotropic lattice correspondence. In this case, a rational OR with parallel C.P planes is normally preferred to enable the singular interface or facet defined by a $\Delta\mathbf{g}$ vector that is parallel to one of the C.P planes of the nanowires, following the first optimum condition. At such an interface, the misfit strain is not confined along the matching rows any more. The strain relaxation will follow either V-W or S-K mode if the substrate is parallel to the singular interface while an endotaxy fashion will be favored if the singular interface is inclined to the substrate, as can be seen in Fig. 4(b).

click for feedback
consult - comment - contact

click for feedback
consult - comment - contact

Summary

The natural preference of either rational OR with low-indexed interface or crystallographic tilting with high-indexed interface must be associated with one of the local cusps of the interfacial energy, in 5-D boundary geometrical phase. The latter mode is usually preferred when atomic row matching can be realized across the interface to relax the long-range strain. In this case, the OR and interface orientation can be fully described by the E2EM model in combination with $\Delta\mathbf{g}$ parallelism rules II or III. In contrast, the former mode is normally preferred when atomic row matching is not achievable subject to the transition strain tensor. In this case, the E2EM model is not applicable, but $\Delta\mathbf{g}$ parallelism Rule I can always be used to define the OR and singular interface.

References

[1] J.E. Ayers: *Heteroepitaxy of Semiconductors: Theory, Growth, and Characterization* (Taylor & Francis Group, New York 2007).

[2] M. Volmer and A. Weber: Z. Phys. Chem. Vol. 119 (1926), p. 277

[3] I.N. Stranski and Von L. Krastanow: Akad. Wiss. Lit. Mainz Math.-Natur. Kl. IIb Vol. 146 (1939), p. 797

[4] J. H. Claassen, S. A. Wolf, S.B. Qadri, *et al*: J. Cryst. Growth Vol. 81 (1987), p. 557

[5] M. Shigeta, Y. Fujii, A. Ogura, *et al*: J. Cryst. Growth Vol. 93 (1988), p. 766

[6] J. Plitzko, M. Rösler and K.G. Nickel: Diam. Relat. Mater. Vol. 6 (1997), p. 935

[7] F. Riesz, J. Varrio, A. Pesek, *et al*: Appl. Surf. Sci. Vol. 75 (1994), p. 248

[8] M. Peruzzil, J.D. Pedarnig, D. Bäuerle *et al*: Appl. Phys. A Vol. 79 (2004), p. 1873

[9] Z-A. He, D.J. Smith and P.A. Bennett: Appl. phys. Lett. Vol. 86 (2005), 143110

[10] A. Riemann, S. Fölsch and K.H. Rieder: Phys. Rev. B Vol. 72 (2005), 125423

[11] W-Z. Zhang, in: *Proc of 4th Inter. Conf. on Solid-Solid Phase Transformations,* edited by M. Koiwa, K. Otsuka and T. Miyazaki. Japan Inst. of Metals (1999), p. 581

[12] W-Z Zhang and G.C. Weatherly: Prog. Mater. Sci. Vol. 50 (2005), p. 181

[13] P.M. Kelly and M-X Zhang: Mater. Forum Vol. 23 (1999), p. 41

[14] P.M. Kelly and M-X Zhang: Metall. Mater. Trans. A Vol. 37A (2006), p. 833

[15] K. N. Tu, R.D. Thompson and B.Y. Tsaur: Appl. Phys. Lett. Vol. 38 (1981), p. 626

[16] Z. He, D.J. Smith and P.A. Bennett: Appl. Phys. Lett. Vol 86 (2005), 143110

[17] Z. He, D.J. Smith and P. A. Bennett: Phys. Rev. B Vol. 70 (2004), 241402

[18] G. Ye, J. Nogami and M.A. Crimp: Thin Solid Films Vol. 497 (2006), 48

[19] J. Nogami, B.Z. Liu, M.V. Katkov, *et al*: Phys. Rev. B Vol. 63 (2001), 233305

[20] C. Preinesberger, S.K. Becker, S. Vandre, *et al*: J. Appl. Phys. Vol 91 (2002), 1695

[21] Z. He, D.J. Smith and P.A. Bennett: Appl. Phys. Lett. Vol 83 (2003), 5292

[22] M-X. Zhang and P. M. Kelly: Scripta. Mater. Vol 52 (2005), 963

[23] W-Z. Zhang, F. Ye, C. Zhang, Y. Qi and H-S. Fang: Acta Mater. Vol. 48 (2000), p. 2209

[24] J. Wu, W-Z. Zhang, X-F. Gu: Acta Mater. Vol. 57 (2009), p. 635

[25] F. Ye and W-Z. Zhang: Acta Mater. Vol. 50 (2002), p. 2761

[26] D. Qiu, P.M. Kelly and M-X. Zhang: Scripta Mater. Vol. 60 (2009), p. 787

[27] Z. He, D.J. Smith and P.A. Bennett: Phy. Rev. Lett. Vol. 93 (2004), 256102

consult
comment
contact
click for feedback

Solid-Solid Phase Transformations in Inorganic Materials
doi:10.4028/www.scientific.net/SSP.172-174

Heteroepitaxy Crystallography in Low Dimensional Nanostructures
doi:10.4028/www.scientific.net/SSP.172-174.1307

click for feedback
consult - comment - contact

consult
comment
contact
click for feedback